



An Investigation on Effect of Shell Liner Type on Performance of Industrial SAG Mills Using DEM

M. Jahani Chegeni* and S. Kolahi

Faculty of Mining, Petroleum & Geophysics Engineering, Shahrood University of Technology, Shahrood, Iran

Received 22 October 2019; received in revised form 29 January 2020; accepted 7 February

Keywords

DEM simulation
Industrial SAG mills
Mill shell liner type
Head height
Impact zone length

Abstract

The shell liner type, rotation speed, and ball filling percent are the key factors influencing the charge behavior inside the SAG mills, and consequently, their performance. In this work, the milling operation of industrial SAG mills is investigated using the Discrete Element Method (DEM). First, an industrial SAG mill with dimensions of $9.50 \text{ m} \times 4.42 \text{ m}$ that has a Smooth-type liner is simulated. Then by changing the liner types, i.e. Wave, Rib, Ship-lap, Lorain, Osborn, and Step liners, six other independent simulations are performed. In order to investigate the impact mechanism and improve the mill performance, two new parameters called 'head height' and 'impact zone length' are introduced. Then the effects of the mill shell liner type on those parameters at two different mill speeds, i.e. 70% and 80% of its critical speed (CS), are evaluated. Also for validation of the simulation results, a laboratory-scale SAG mill with dimensions of $57.3 \text{ cm} \times 16.0 \text{ cm}$ is simulated. The results obtained indicate that the Osborn liner, due to the angularity of its lifters and their proper number and thickness, performs best because it increases both parameters more than the other liners. Thus this liner is recommended as the best and optimal liner in this research work and is suggested for installation inside the industrial SAG mills. Also the Wave liner, due to its specific geometrical shape and its wavy lifters as well as their low number and inadequate thickness, provides the lowest charge 'head height'. Therefore, it is not recommended to install this liner inside the industrial SAG mills. Meanwhile, comparison of the simulations related to the laboratory-scale SAG mill with the experimental results demonstrates a good agreement that validates the DEM simulations and the software used.

1. Introduction

Grinding is the most common process used to liberate the valuable minerals from the gangue. Tumbling mills have been used mainly in the mineral processing industry since the mid-19th century due to the need for finer materials. However, there is still a need for understanding the combined and individual effects of all the design and operating variables to make the process more efficient [1]. Mishra and Rajamani [2] were the first ones to track the motion of the ball charge in large-diameter ball mills using Discrete Element Method (DEM) simulation. Later, Powell and McBride [3] illustrated the media motion and grinding regions (head, departure shoulder, center

of circulation, equilibrium surface, bulk toe, and impact toe). In the last three decades, the importance of lifter in the charge behavior in tumbling mills has been discussed. Cleary [4, 5] has used DEM to predict the wear of lifters and the power draw of SAG mills. Examples of 3D models of SAG mills have been presented by Cleary [6]. Comparisons of the simulation results with the photographs of charge motion in a scale model SAG mill demonstrate a high degree of accuracy. Predictions of flow patterns in a 600-mm scale model SAG mill was made using four classes of DEM models, and were compared with the experimental photographs by Cleary *et al.* [7]. The

shoulder, toe, and vortex center positions were measured both experimentally and by DEM simulation. In particular, very close agreement was demonstrated between the full 3D model (including the end wall effects) and the experiments. It was also demonstrated that the traditional 2D circular particle DEM model under-predicted the shoulder, toe, and vortex center positions by around 10 degrees [7]. DEM has been used by Djordjevic *et al.* [8] to model the effects of lifter height (5–25 cm) and mill speed (50–90% of critical) on the power draw and frequency distribution of specific energy (J/kg) of normal impacts in a 5 m diameter autogenous (AG) mill. It was found that the distribution of the impact energy was affected by the number of lifters, lifter height, mill speed, and mill filling. By gradually increasing the tumbling model SAG mill length and analyzing the charge trajectory and shape variation at given operating conditions (i.e. ball filling, mill speed, liner type), the impact of end-wall effect on the charge trajectory in model mills has been investigated by Maleki-Moghaddam *et al.* [9]. Four types of liners, five steel ball fillings (10, 15, 20, 25, 30% v/v), and three mill speeds (55%, 70%, 85% of critical speed) were tested. The results obtained indicated that when the mill length was below 10.8 cm, the end-walls prevented the charge from free falling. This resulted in lower impact point angles and lower power draws compared to the case of no end-wall effect [9]. A relationship between charge shape characteristics and fill level and lifter height for a SAG mill has been obtained by Owen and Cleary [10]. A predictive model that allows the mill fill level and the lifter height to be determined from measurements of the head, bulk, and impact toe positions for a generic SAG mill was developed using the data from a series of 3D DEM simulations. A Design of Experiment (DOE) approach was used to define a series of simulation conditions with the two factors being the lifter height and the fill level. The charge structure was characterized by the locations of the head, shoulder, bulk toe, and impact toe. These were determined by the visual analysis of the particle trajectories [10]. Estimating energy in grinding using DEM modeling has been conducted by Weerasekara *et al.* [11]. They developed a series of DEM models that allowed simulating charge motion in SAG mills ranging from pilot-scale to industrial-scale with a varied mill load. The characteristic charge structures for this study were estimates for the head, shoulder, bulk toe, and impact toe, together with the analysis of the DEM modelled breakage energy environment for

multiple scales of mills [11]. A set of 22 3D DEM simulations have been conducted by Cleary and Owen [12] to understand and quantify the relationship between the key charge locations and the three important operating parameters—fill level, lifter height, and mill speed for a generic SAG mill. The charge shape and location were characterized by the shoulder, head, bulk, and impact toe positions, and were assessed by analysis of particle trajectories and the spatial variation of the pressure on the liner. They also explored how such parametric models could be used to create the operational management strategies (in terms of how to vary the control variables such as the target mill fill level and mill speed) [12]. The role of end liners in dry SAG mills with the objective of obtaining a thorough understanding of the effects of end liners design on the load trajectory and SAG mill performance has been studied experimentally by Hasankhoei *et al.* [13]. The test works were conducted in a scale-down mill with a diameter of 1 m. It was shown that the liner in the first and the last 20% of the mill length that were under the protection of the deflector liners experienced no deformation [13].

Grinding consumes most of the energy in mineral processing. The SAG mill is an important kind of grinding equipment used to decrease the size of ore particles. The power consumption of a SAG mill is one of the most important parameters to consider in the design of a SAG mill because it determines its economic efficiency. The power consumption is usually determined by the charging fill level, lifter height, lifter number, and mill speed. However, almost all of the classical theories for calculating the power consumption of SAG mills disregard the effect of lifters, and only focus on the rotation rate and charge fill level as well as the size and shape of grinding media, and thereby, may cause errors [14]. Mill liners protect mill shells from abrasion and lift ore particles and grinding media to a high position. Therefore, liners/lifters must be able to bear high-impact loads during the grinding process. The wear rate of these components is high, and these parts tend to break or incur wear-out failure, which can seriously affect the production efficiency of SAG mills. Thus the research on liner structure and configuration of SAG mills is crucial to improve the production ability and economy of SAG mills [14].

The mineral processing industry could save about 70% of the power involved in grinding processes if this power was reduced to its practical minimum power consumption [15]. In this context, achieving a more efficient grinding in SAG mills is an

important issue since they have a low efficiency rate, partially due to the lack of creation of cascading and cataracting motions for balls and inappropriate shoulder and toe points [16]. For a given number of balls, if the mill rotation speed is higher than or equal to its critical speed, the balls stick to the mill wall and the grinding operation does not occur, and centrifuging motions are created. On the other hand, if the mill speed is between 80% and 100% of its CS, the suitable shoulder and toe points are not created, and the grinding energy is used to hit the balls with the mill wall; in this mode, centrifuging motions are also created. However, if the mill speed is between 60% and 80% of its CS, the appropriate shoulder and toe points as well as the cascading and cataracting motions are created, which result in better grinding. In this case, the dominant mechanism will be impact, which is the optimum mode for the process, and will reduce the power consumption of the mill. Meanwhile, the abrasion mechanism is not very effective in this mode. At speeds less than 60% of CS, the cascading and cataracting motions gradually disappear and the balls roll over each other. In this case, grinding is not optimal and the abrasion mechanism plays a more effective role [16]. Among the other effective factors on creating cascading and cataracting motions in mills, lifters can be mentioned. Lifters cause the balls to climb to a higher elevation and prevent their slipping [16].

According to the research work conducted and is ongoing by the authors of this article, in the curved and smooth angled liners, due to their appearance, the cataract motions are not created properly and the balls slide over each other. As a result, the abrasion mechanism on these liners is more than the other liners. Therefore, to make cataract motions in them, it is necessary to increase the mill speed. However, in the edged and angled liners, the appropriate cataract motions are created. Thus the impact mechanism on these liners is more dominant. Therefore, the optimum speed of the mills with these types of liners can be chosen less than the previous ones. Another important issue with the mill liners is the number of lifters and their thickness. According to our previous research work, the optimum number of lifters for ball mills is between 8 and 32 lifters, and for SAG mills is between 16 and 64 lifters with a medium thickness. Liners with a number of lifters in this range require less mill speed to create cataract motions. However, liners with a number of lifters less than this range require a higher mill speed. Also liners with a number of lifters beyond this range require

less mill speed, and they can cause centrifugal motions in the balls.

Simulation has become a common tool in the design and optimization of industrial processes [17]. The continuous increase in computing power has now enabled the researchers to implement the numerical methods that do not focus on the granular assembly as an entity but rather deduce its global characteristics from observing the individual behavior of each particle [17]. Due to their discontinuous nature, one should expect that granular media require a discontinuous simulation method. Indeed, to date, DEM is the leading approach to those problems [17]. Due to its inherent advantages in analyzing granular materials, DEM has been developed rapidly in the recent decades and is used widely in mineral processing engineering [17].

In order to control, optimize, and reduce the SAG mill power consumption, the mineral processing engineers must obtain enough information about their operation conditions. One of the most effective techniques is the use of computer simulations. Computer simulations using methods such as DEM can be effective to find optimal speed of SAG mills, and as a result, create appropriate shoulder and toe points in them as well as creating cascading and cataracting motions. This method can also be used to prevent centrifugal motions. In this research work, DEM is introduced and used, utilizing an open-source software, LIGGGHTS, to simulate the milling operation of the industrial-scale SAG mills. An industrial-scale SAG mill with a Smooth liner type is simulated. Then by changing the liner type, i.e. Wave, Rib, Ship-lap, Lorain, Osborn, and Step liners, six other independent simulations are performed. Also, in this paper, it has been shown that 'shoulder height' and 'toe height', which are used in all the previous investigations by the researchers to evaluate and determine the trajectory of ball motion, are not suitable criteria for investigating the impact mechanism and improving the mill performance. For this reason, for the first time, two new parameters called 'head height' and 'impact zone length' are introduced by the authors instead of them. The charge head height means the highest altitude when the particles begin to detach from the mill and begin their cataracting motion. Also the impact zone length is the difference of the length of the toe point with the highest end point of the cataract motion (impact point) (Figure 1). Additionally, the effects of the mill shell liner type on charge shoulder, toe, impact, and head points, also on head height and impact zone length as well

as on creation of cascading, cataracting, and centrifuging motions for balls at two different mill speeds, i.e. 70% and 80% of its critical speed (CS), are evaluated. Also in order to validate the simulation results, a laboratory-scale SAG mill is simulated. In summary, in this research work, for the first time, the effects of different mill liner types on two new parameters introduced by the authors, i.e. ‘head height’ and ‘impact zone length’, and as

a result, on the impact mechanism and performance of industrial-scale SAG mills at different mill speeds (70% and 80% of CS) using discrete element method are investigated. The main innovation and novelty of this work is introducing and basing ‘head height’ and ‘impact zone length’ to evaluate and determine the trajectory of ball motion for investigating the impact mechanism and improving the mill performance.

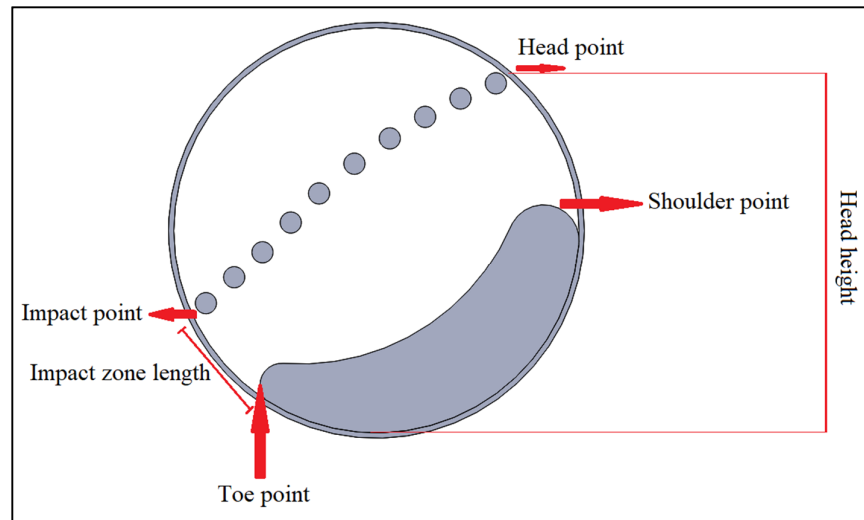


Figure 1. Charge head, shoulder, toe, and impact points as well as head height and impact zone length.

2. Simulation method

2.1. Use of DEM to predict particle flow

DEM is a numerical technique used to predict the behavior of collision dominated particle flows. Each particle in the flow is tracked, and all collisions between particles and between particles and boundaries are modeled. DEM is a powerful numerical tool for simulating the mechanical behavior of systems with a large number of particles based on particles' motion and interactions and their representation as rigid geometric bodies, commonly having a spherical shape [18, 19], whereas simulations with spherical particles can include millions of particles using non-spherical particles is still not an easy task; for spherical particles, the geometry is described by the radius and the interaction forces that can be easily calculated by contact laws like Hertzian contact. For non-spherical particles, the geometry representation and calculation of contact forces are much more complex [18, 20]. DEM is based on the Lagrangian approach and treats granular materials as an assemblage of distinct particles, each governed by physical laws [21, 22]. Each particle interacts with its neighbors through particle-to-particle contacts, which can be formed or broken at each time step [19, 21, 23–25]. In the recent years,

the drastic increase in the affordable computational power has allowed DEM simulations to become a versatile tool for industrial applications [26]. The recent advances in the discrete element modeling have resulted in this method becoming a useful simulation tool that can provide detailed information, not easily measured during experiments [27]. With the maturing of DEM simulation, it has now become possible to run simulations of millions of particles with complex shapes and inter-particle cohesive forces in tolerable times on the single processor, desktop computers [17, 26–28].

In this research work, an open-source software, LIGGGHTS, was used to perform DEM simulations. The DEM variant used here is sometimes called a ‘soft particle method’. The particles are allowed to overlap, and the extent of overlap is used in conjunction with a contact force law to give instantaneous forces from knowledge of the current positions, orientations, velocities, and spins of the particles [29]. Here, we used the Hertz–Mindlin's contact force law. It states that the repulsive force resulting from a collision is calculated from the amount of normal overlap δ_n and tangential overlap δ_t (soft-sphere approach) [30]. This granular model uses the following

formula for the frictional force between two granular particles when the distance r between two particles of radii R_i and R_j is less than their contact distance $d = R_i + R_j$ (in this formula, the vector parameters are written in bold and the scalar ones are written in normal text). There is no force between the particles when $r > d$:

$$F = (k_n \delta n_{ij} - \gamma_n v n_{ij}) + (k_t \delta t_{ij} - \gamma_t v t_{ij}) \quad (1)$$

The first term is the normal force (F_n) between the two particles, and the second term is the tangential

force (F_t). The normal force has two terms: a spring force and a damping force. The tangential force also has two terms: a shear force and a damping force. The shear force is a “history” effect that accounts for the tangential displacement (tangential overlap) between the particles for the duration of the time they are in contact.

The quantities in the equation are as follow:

-
- k_n : elastic constant for normal contact;
 - δn_{ij} : $d - r =$ normal overlap (overlap distance between the two particles);
 - γ_n : viscoelastic damping constant for normal contact;
 - $v n_{ij}$: normal relative velocity (normal component of the relative velocity of the two particles);
 - k_t : elastic constant for tangential contact;
 - δt_{ij} : tangential overlap (tangential displacement vector between the two spherical particles, which is truncated to satisfy a frictional yield criterion);
 - γ_t : viscoelastic damping constant for tangential contact;
 - $v t_{ij}$: tangential relative velocity (tangential component of the relative velocity of the two particles).
-

Considering that the shear modulus (G) can be calculated from the Young's modulus and Poisson ratio, the Hertz–Mindlin contact model depends on the following material parameters [30]:

-
- Coefficient of restitution, e ;
 - Young's modulus, Y ;
 - Poisson ratio, ν ;
 - Coefficient of static friction, μ_s ;
 - Coefficient of rolling friction, μ_r .
-

The maximum overlap between particles is determined by the stiffness k_n of the spring in the normal direction. Typically, the average overlaps of 0.1–0.5% are desirable, requiring spring constants of the order of 10^4 – 10^6 N/m in three dimensions. The normal damping coefficient γ_n is chosen to give the required coefficient of restitution e (defined as the ratio of the post-collisional to pre-collisional normal component of the relative velocity) [31].

In DEM, the particles are traditionally approximated by disks or spheres in two and three dimensions, respectively. These shapes are preferred due to their computational efficiency. The contact is always on the line joining the center of each particle, and is as simple as comparing the distance between their centers to the sum of their radii [42, 44]. Since in SAG mills the balls are spherical, DEM can be appropriately used to simulate their motion.

The drawback of DEM is that the time step has to be chosen extremely small because the contact force exhibits a very stiff behavior. Depending on

the material properties and the particle size, the time step size can be as low as 10^{-6} s for an accurate simulation [32–34].

In this work, the time step was calculated according to the Rayleigh time step, which is the time a shear wave requires to propagate through a solid body. In order to fully resolve the whole process, 20% of it was used as the time step for the simulations (Δt). The Rayleigh time step could be determined using the smallest couple of the particle radius r (6 cm), its density ρ (8,050 kg/m³), shear modulus G (0.389 GPa), and Poisson ratio ν (0.285):

$$\Delta t = 0.20 \times \frac{\pi r \sqrt{\rho/G}}{(0.1631\nu + 0.8766)} = 0.0001858 \approx 0.0002 \quad (2)$$

The relationship between the modulus of elasticity (E) (Young's modulus) (Y) (1 GPa) and the shear modulus (G) is as follows:

$$G = \frac{E}{2 \times (1 + \nu)} = \frac{1 \times 10^9}{2 \times (1 + 0.285)} = 0.389 \text{ GPa} \quad (3)$$

3. SAG mill configuration

In this work, an industrial-scale SAG mill with no lifter was simulated by the DEM method. Then by changing the liner type, i.e. Wave, Rib, Ship-lap, Lorain, Osborn, and Step liners, six other independent simulations were performed (Figure 2). It is worth noting that the liner types used in this work were selected based on the dimensions available in Figure 7.11 of the B. A. Wills' book [16] and drawn using reverse engineering.

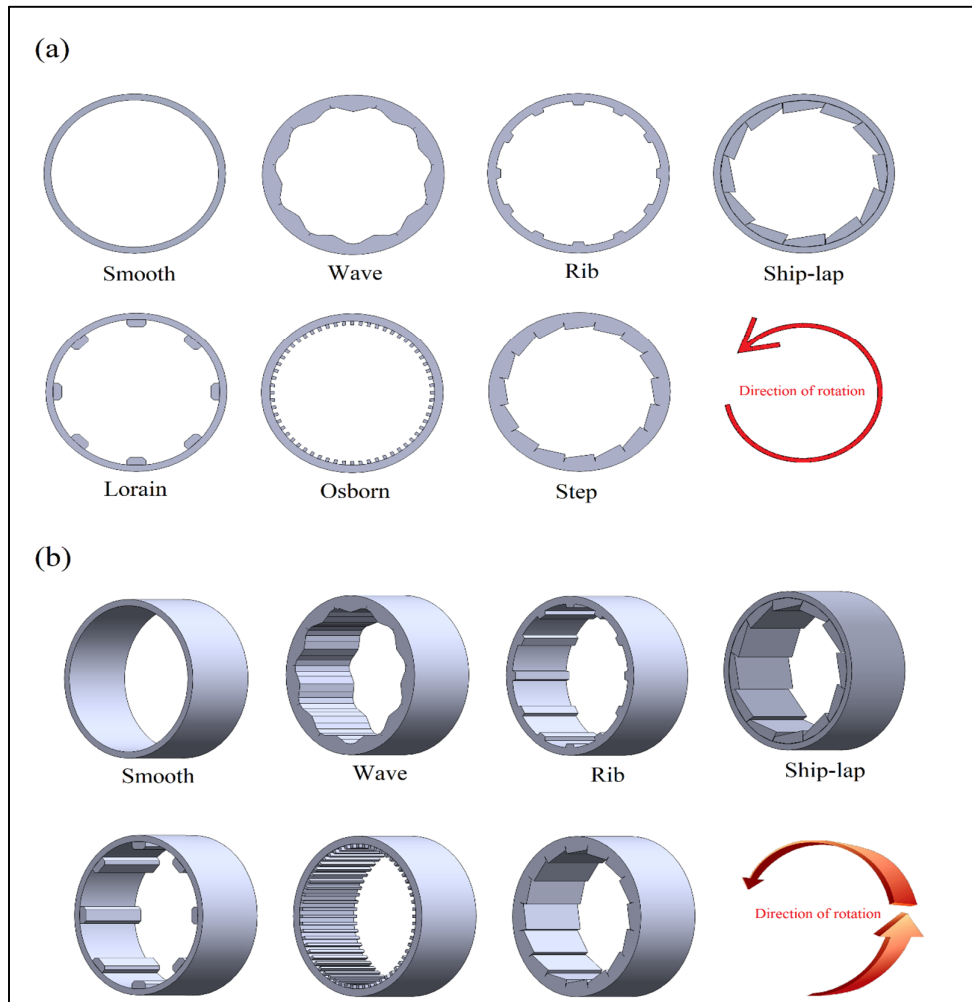


Figure 2. 2D (a) and 3D (b) geometries of industrial SAG mills with different liner types.

The detailed geometrical and operational conditions and material properties and calculations for these industrial SAG mills are listed in Tables

1–3. It should be noted that the material of the SAG balls used in the simulations was stainless steel.

Table 1. Industrial SAG mill dimensions and speeds.

Industrial SAG mill	Dimensions	
Smooth mill shell thickness (cm)	40	
Mill length (m)	4.42	
Mill diameter (m)	9.50	
Mill volume at smooth mode (m ³)	313.2993	
CS (critical speed) (rpm)	13.81	
Direction of rotation of mill	Counter-clockwise	
Minimum & Maximum thickness of Wave liner (cm)	20	60
Number of lifters of Wave liner and spacing between them (cm)	11	0.7
Minimum & Maximum thickness of Rib liner (cm)	25	25
Number of lifters of Rib liner and spacing between them (cm)	12	175
Minimum & Maximum thickness of Ship-lap liner (cm)	33.5	67.4
Number of lifters of Ship-lap liner and spacing between them (cm)	12	5
Minimum & Maximum of Lorain liner (cm)	51.1	51.1
Number of lifters of Lorain liner and spacing between them (cm)	8	260
Minimum & Maximum thickness of Osborn liner (cm)	25	25
Number of lifters of Osborn liner and spacing between them (cm)	60	31
Minimum & Maximum thickness of Step liner (cm)	31	54.8
Number of lifters of Step liner and spacing between them (cm)	16	0.5

Table 2. DEM ball Size distribution and specification.

Ball size class (cm)	Mass fraction (%)
12	100

Table 3. Parameters used and calculated for the DEM simulations of the industrial SAG mill.

DEM model details	Value
Ball diameter (mm)	120
Volume of one ball (m ³)	9.0478 × 10 ⁻⁴
Mill filling percent (%)	15
# Balls	23.4974/9.0478 × 10 ⁻⁴ = 25970.37 ≈ 25970
Ball density (kg/m ³)	8050
Mass rate (ton/s)	18.915 (10 steps)
Neighbor (particle interaction distance) (m)	5% × 60 mm = 3 × 10 ⁻³
Total mass of ball charge (kg)	189154.43
DEM spring constant (kg/m)	10 ⁶
Ball sliding friction coefficient	0.5
Ball rolling friction coefficient	0.0015
Poissons ratio	0.285
Young's modulus (N/m ²)	1×10 ⁹
Ball restitution coefficient	0.817
Time step (s)	0.0002

4. Results and discussion

Figures 3 and 4 demonstrate the front view and isometric view of 3D snapshots of the simulations of the industrial SAG mills with the different liner types Smooth, Wave, Rib, Ship-lap, Lorain,

Osborn, and Step, respectively, when the drum is rotating at 70% and 80% of its CS using DEM. As it can be seen, in all the liner types, the cascade motion is observed at both mill speeds.

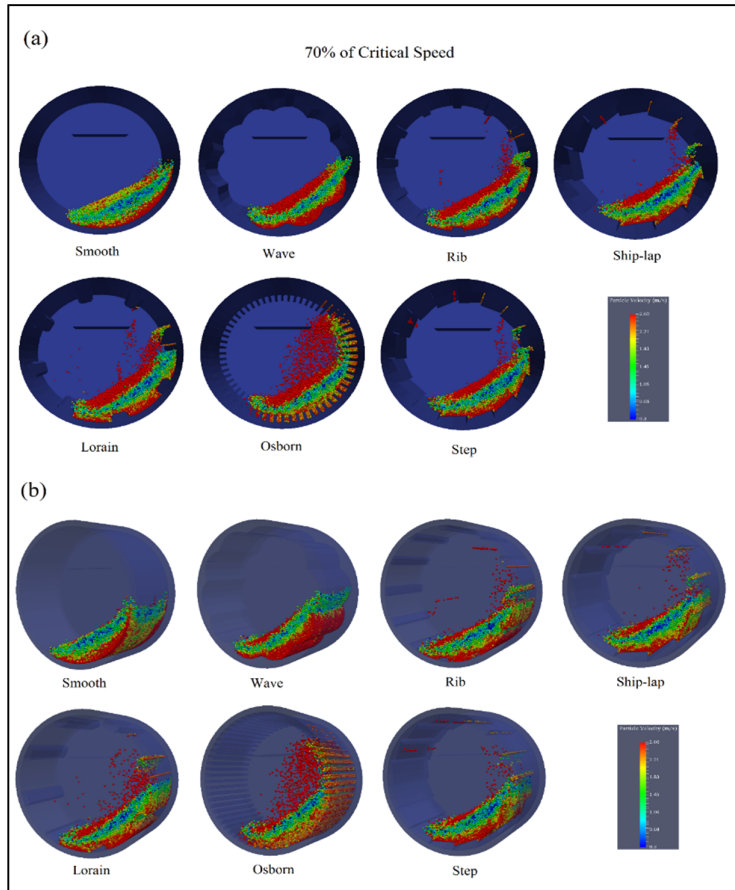


Figure 3. Front view (a) and isometric view (b) of 3D snapshots showing the motion of particles on the industrial SAG mills with different liner types at 70% of CS using DEM.

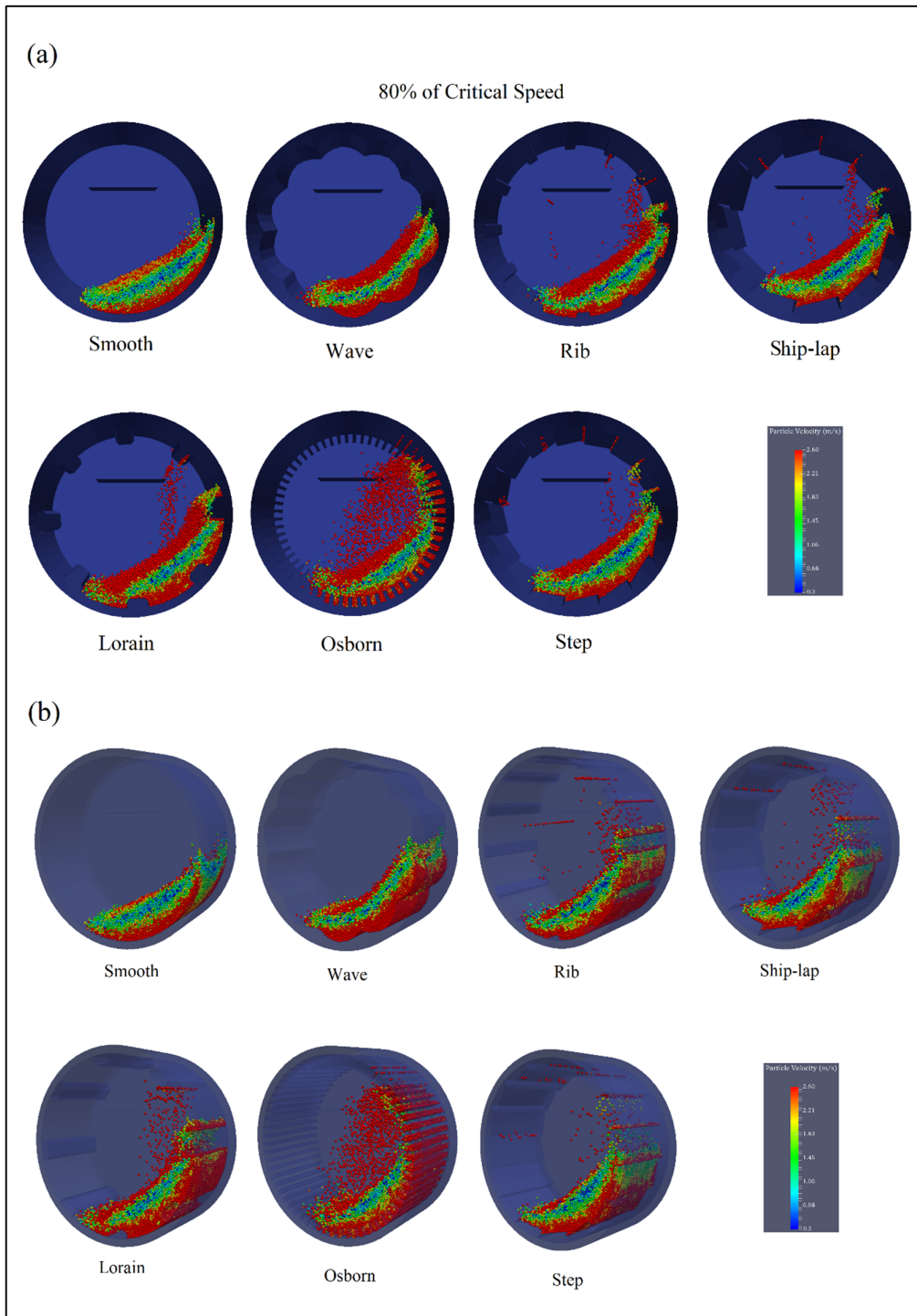


Figure 4. Front view (a) and isometric view (b) of 3D snapshots showing the motion of particles on the industrial SAG mills with different liner types at 80% of CS using DEM.

Figure 5 demonstrates how to measure the angle of the charge shoulder, toe, and head points (degree) as well as the impact zone length (cm) using an online protractor in the industrial SAG mills with the different liner types Smooth, Wave, Rib, Ship-lap, Lorain, Osborn, and Step, respectively, when the drum is rotating at 70% (a) and 80% (b) of its

CS using DEM. The exact values of the height (cm) and angle (degree) of the shoulder, toe, and head points as well as the impact zone length (cm) of the balls for the industrial SAG mills with the different liner types of Smooth, Wave, Rib, Ship-lap, Lorain, Osborn, and Step at different drum speeds are available in Table 4.

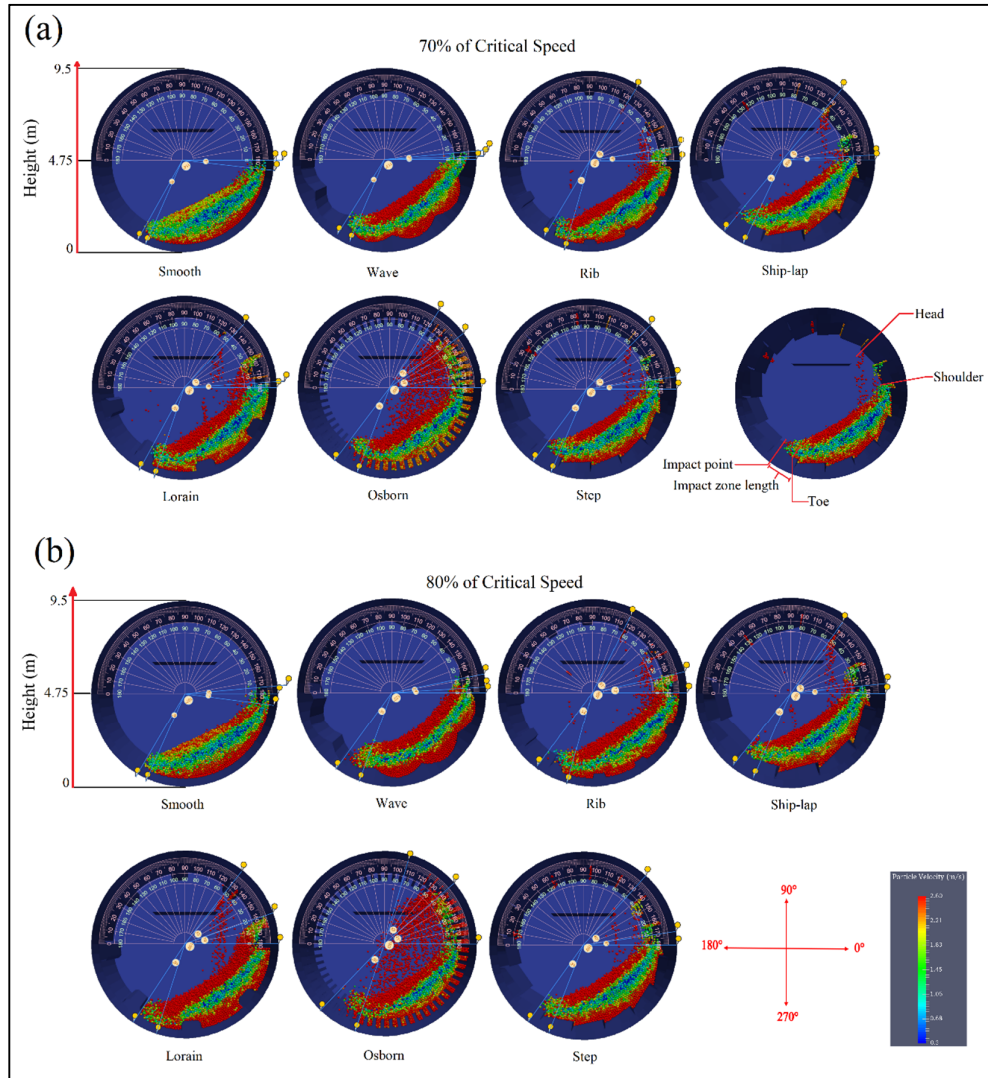


Figure 5. Using an online protractor to determine the height (cm) and angle (degree) of the shoulder, toe, and head points as well as the impact zone length (cm) in the industrial SAG mills.

Table 4. Values of the height and angle of the shoulder, toe, and head points as well as the impact zone length of the balls for the industrial SAG mills with different liner types.

Mill liner type	CS (%)	Cataract motion	Centrifuge motion	Head height (cm)	Shoulder height (cm)	Toe height (cm)	Impact zone length (cm)
Smooth	70	no	no	475.00	425.35	23.25	49.72
Wave	70	no	no	516.40	491.58	44.50	74.54
Rib	70	yes	no	873.37	549.31	18.40	124.00
Ship-lap	70	yes	yes	838.87	499.86	44.50	115.78
Lorain	70	yes	no	822.39	508.13	25.88	82.80
Osborn	70	yes	no	877.82	760.86	31.55	132.21
Step	70	yes	yes	810.88	541.11	37.76	107.54
Smooth	80	no	no	516.40	417.11	10.38	49.72
Wave	80	no	no	573.76	508.13	28.65	132.21
Rib	80	yes	no	901.93	581.85	16.19	173.12
Ship-lap	80	yes	yes	859.28	524.65	37.76	124.00
Lorain	80	yes	no	849.31	629.64	20.76	132.21
Osborn	80	yes	no	931.60	786.63	25.88	205.62
Step	80	yes	yes	828.00	541.11	31.55	115.78

At first glance, the results of Figure 5 and Table 4 may seem simple software outputs from DEM. However, after simulations, all the required information is available on the motion of all individual particles so that the researcher (computer user) can examine the position of each individual particle and its motion, which leads to the identification of charge head, shoulder, toe, and impact points, which was the main purpose of this work.

The following results are obtained from Table 4: in all liners at both speeds (70% and 80% of CS), the cascade motion is observed. At 70% and 80% of CS, the Smooth and Wave liners do not produce cataracting motion. At 70% and 80% of CS, the centrifugal motion is only available for the Ship-lap and Step liners. As a result, some of the balls do not participate in the comminution, and the impact mechanism will be reduced. In other liners, a cataract motion is observed. At 70% of CS, the highest head height and shoulder height are, respectively, 877.82 and 760.86 cm for the Osborn liner. Also the maximum impact zone length is 132.21 cm for this liner. However, the maximum toe height belongs to the Wave and Ship-lap liners (44.50 cm). At 80% of CS, again the highest head height and shoulder height are, respectively, 931.60 and 786.63 cm for the Osborn liner. Also the maximum impact zone length is 205.62 cm for this liner. However, the maximum toe height belongs to the Ship-lap liner (37.76 cm). By comparing the values of head height and shoulder height, it can be concluded that the shoulder height does not follow a certain rule so it cannot be used as an appropriate criterion for evaluating the impact mechanism and comminution performance of the mill. For this reason, 'head height' has been replaced as an evaluation criterion, and is used in this work as a suitable criterion. Also the toe height values do not follow a specific rule so the toe height cannot be used as an appropriate criterion for evaluating the mill performance. Consequently, in this work, the 'impact zone length' has been selected and replaced as another suitable criterion for evaluation of the mill performance. In this work, contrary to the previous works, in which shoulder and toe heights were considered as the basis for investigating the impact mechanism and mill performance, for the first time, charge 'head height' and 'impact zone length' are considered as the main criteria for evaluating the impact mechanism and mill performance. Therefore, the values for these two parameters are shown in

capital letters in Table 4. Further results from Table 4 are shown in Figure 6.

Figure 6 shows the effect of mill shell liner types on charge head height and impact zone length of industrial SAG mills at 70% and 80% of CS. As it can be seen, at 70% of CS, the Rib and Osborn liners perform best and increase the charge head height dramatically. However, the Wave liner, due to its appearance (its specific geometrical shape and its wavy lifters as well as their low number and inadequate thickness), increases the wear mechanism, resulting in a poor performance, and acts almost like the Smooth liner. Overall, at 70% of CS, all liners except the Wave Liner have a favorable effect on the impact mechanism. Also the Osborn, Rib, Ship-lap and Step liners, respectively, have the greatest effect on the impact zone length and improvement of the impact mechanism and mill performance. However, the Lorain and Wave liners do not have a significant effect on the impact zone length. Overall, at 70% of CS, the Osborn liner (due to the angularity of its lifters and their proper number and thickness) performs best because it increases both the charge head and the impact zone length. At 80% of CS similar to the 70% of CS state, the Osborn and Rib liners have again produced the highest charge head height but the Wave liner does not have a favorable effect on the charge head. Generally, at 80% of CS, all liners except Wave liner have a favorable effect on increasing charge head height. Also the Osborn and Rib liners have the most positive effect on the impact zone length, and thereby, enhance the impact mechanism and improve the mill performance. Unlike the 70% case, the Wave and Lorain liners also have a relatively favorable effect on increasing the impact zone length. Overall, at 80% of CS, the Osborn and Rib liners have the best performance and the other liners have a relatively successful performance in increasing the impact zone length. Also at 80% of CS, the Osborn liner is recommended as the best liner because it increases both the charge head height and the impact zone length.

On the other hand, Figure 6 shows the effects of different types of mill shell liners on increasing the charge head height and impact zone length compared to the Smooth liner at 70% and 80% of CS. At 70% of CS, the Osborn and Rib liners have the highest increase in both cases. As a result, at 70% of CS, these liners are recommended for the mill. The Ship-lap and Step liners also perform relatively well but the Lorain liner only increases the charge head height favorably and does not have a significant effect on the impact zone length. The

Wave liner also lacks the ability to create the right head height and increase of the impact zone length and performs similar to the Smooth liner. In general, at 70% of CS, it can be said that in the Wave liner, the abrasion mechanism is more dominant than the other liners, and therefore, it is not recommended to install this liner in the mineral processing plants. At 80% of CS, the best performance is related to the Osborn liner as it increases both the head height and the impact zone length relative to the other liners so at 80% of CS, this liner is recommended for the mineral processing plant. The Rib liner also performs better than the remaining liners. The rest of the liners have a relatively similar performance in increasing the impact zone length but the Wave liner has little effect on the charge head height so at 80% of CS, this liner is not recommended for the mineral processing plant.

Also Figure 6 demonstrates the effect of mill rotation speed on charge head height for different types of mill shell liners. As it can be observed, in all cases, the increase in critical speed increases the charge head height, and thereby, increases the impact mechanism and improves the mill performance. The most positive effect of increasing the mill speed is on the Osborn, Wave, and Smooth liners. This figure also illustrates the effect of increasing mill speed on the impact zone length for different types of mill shell liners. As it can be seen, in all cases except the Smooth liner, increasing the mill speed increases the impact zone length, and thereby, improves the impact mechanism and mill performance. Also the most

positive effect is related to the Osborn liner. Increasing the mill speed significantly increases the impact zone length on the Wave, Lorain, and Rib liners. However, increasing the mill speed does not have a significant effect on the increase in the impact zone length on the Step and Ship-lap liners. Also increasing the mill speed has no effect on increasing the impact zone length on the Smooth Liner.

If in Figure 6 the effect of mill rotation speed on charge head heights and impact zone lengths for different types of mill shell liners are simultaneously investigated, the following results are obtained. Increasing the mill speed in the Smooth liner only increases the charge head height and does not affect the impact zone length. For the Ship-lap and Step liners, increasing the mill speed has little effect on improving the mill performance. In the Lorain and Rib liners, increasing the mill speed has a greater effect on increasing the impact zone length but has a moderate effect on increasing the head height. Also increasing the mill speed has the most positive effect on the Wave and Osborn liners, with both head height and impact zone length dramatically increase. Although the performance of the Wave liner is not desirable, the effect of speed increase is very effective on improving its performance. As a result, this liner performance can be dramatically improved by increasing the mill speed to values above 80% of CS (e.g. 90% or 95% of CS). In general, according to all conditions, the Osborn liner is preferred over the Rib liner, and is recommended as the optimal liner in this work.

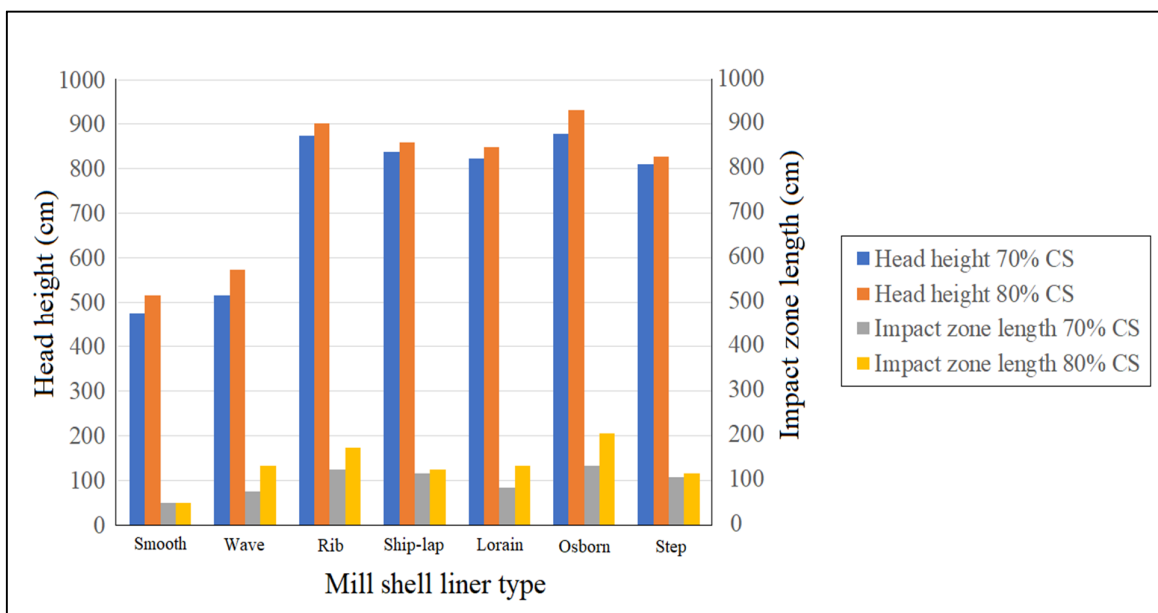


Figure 6. Effect of mill shell liner types on charge head height and impact zone length at 70% and 80% of CS.

4.1. Validation

Since the DEM approach offers such strong advantages in modeling and understanding the milling process, it is essential that both the DEM simulations and the DEM solver are validated properly and adequately. In general, a comprehensive validation of DEM solver and simulations is not feasible and, in most cases, it can be done only partially. In order to ensure the integrity of the application of the DEM techniques to comminution technology and other possible areas, the quality of validation should be improved and directed at the outputs being used in the modeling [35].

In this work, in order to validate the simulation results, a laboratory-scale SAG mill is simulated (Figure 7). The laboratory-scale SAG mill is according to the dimensions described in Bian *et al.* [14]. The detailed geometrical and operational conditions and material properties for the laboratory-scale SAG mill are listed in Tables 5–7, respectively.

In order to validate the obtained results and also the LIGGGHTS DEM solver, charge head height and impact zone length of simulations conducted by this software for the laboratory-scale SAG mill are compared with charge head height and impact zone length of experimental results under the similar conditions (Figures. 8–10 and Table 8). The high agreement between the results indicates their validity and also the validity of the DEM solver.

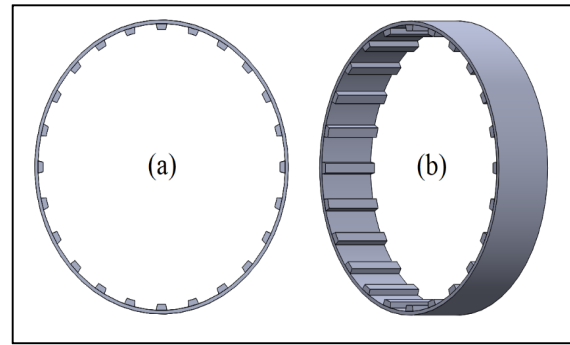


Figure 7. 2D (a) and 3D (b) geometries of the laboratory SAG mill.

Table 5. Laboratory-scale SAG mill dimensions and speeds [14].

Laboratory-scale SAG mill	Dimensions
Shell thickness (cm)	0.75
Mill length (cm)	16
Mill diameter (cm)	57.3
Mill volume (cm ³)	41259
CS (critical speed) (rpm)	56.88
Direction of rotation of mill	Clockwise
Trapezoid lifter length (cm)	16
Trapezoid lifter thickness (cm)	1.20
Trapezoid lifter widths (cm)	1.95 and 2.45

Table 6. DEM ball Size distribution and numbers [14].

Ball size class (mm)	Number of balls	Mass fraction (%)
20	111	5.68
15	795	17.16
13	3051	42.87
8	10474	34.29
Total	14331	100

Table 7. Parameters used for the DEM simulations of the laboratory-scale SAG mill [14].

DEM model details	Value
% Fill of ball charge	40
Total mass of ball charge (kg)	62.8734
DEM spring constant value (kg/m)	10 ⁶
Ball density (kg/m ³)	7800
Ball sliding friction coefficient	0.5
Ball rolling friction coefficient	0.01
Poissons ratio	0.25
Young's modulus (N/m ²)	1×10 ⁹
Ball restitution coefficient	0.5

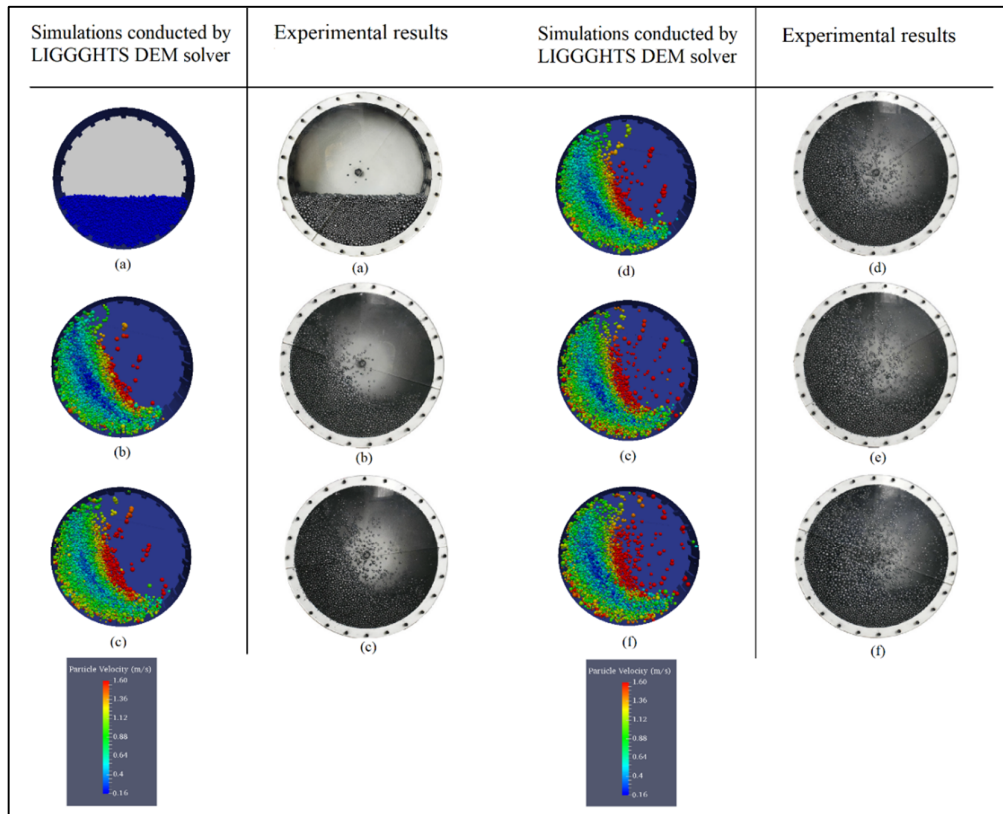


Figure 8. Comparison between simulations of the laboratory-scale SAG mill using LIGGGHTS DEM solver and experimental results [14] at the same operating conditions at (a) 0%; (b) 60%; (c) 70%; (d) 75%; (e) 80%; and (f) 90% of CS.

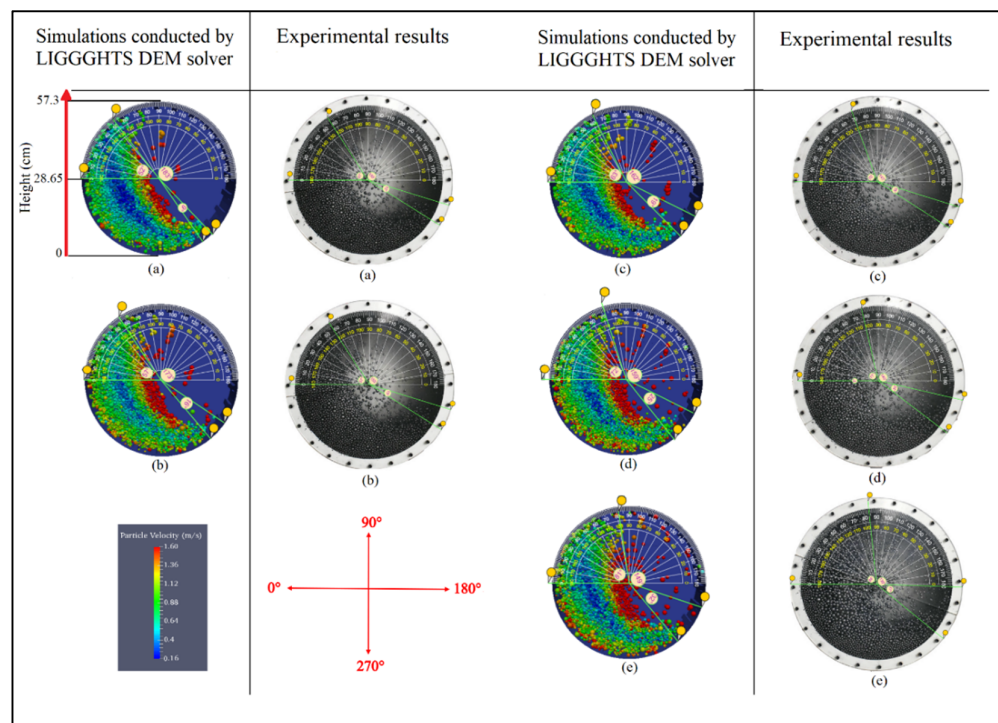


Figure 9. Using an online protractor to determine and compare the charge head height (cm) and impact zone length (cm) of simulations of the laboratory-scale SAG mill and real pictures of experimental results at the same operating conditions at (a) 0%; (b) 60%; (c) 70%; (d) 75%; (e) 80%; and (f) 90% of CS.

Table 8. Comparison of the charge head height (cm) and impact zone length (cm) of simulations of the laboratory-scale SAG mill and real pictures of experimental results [14] at the same operating conditions.

Mill rotation speed (rpm)	Simulations of the laboratory-scale SAG mill		Real pictures of experimental results	
32.79	51.23	4.50	50.92	4.99
38.26	52.68	7.97	52.68	7.48
40.99	54.18	9.46	55.57	7.97
43.72	55.90	12.40	56.57	11.91
49.19	56.95	15.79	57.14	18.18

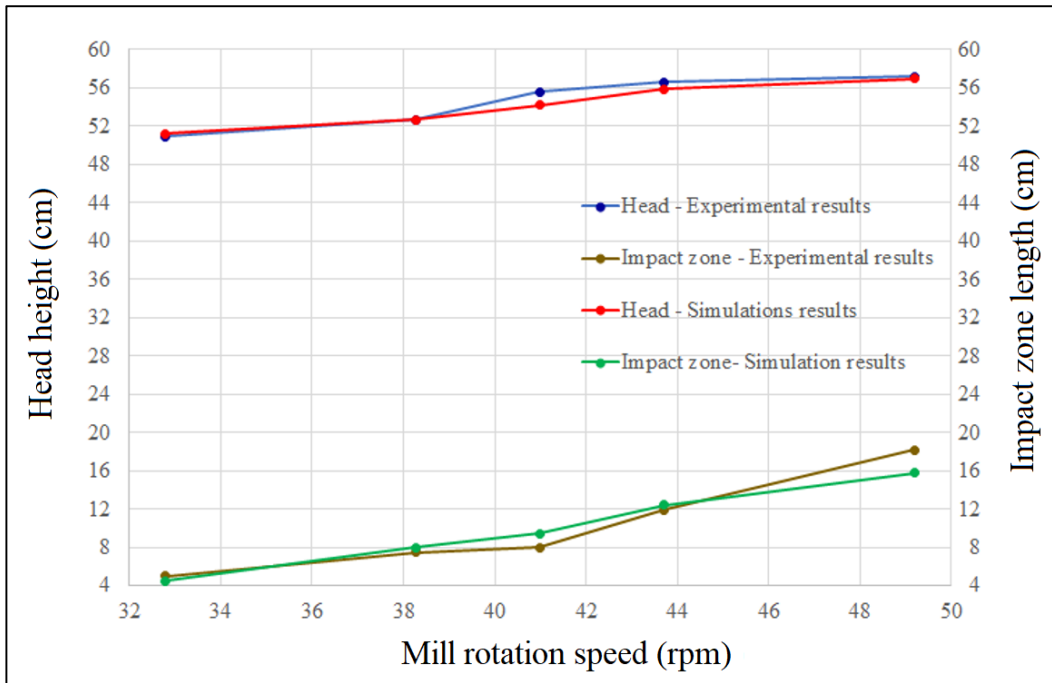


Figure 10. Validation of simulation results of the laboratory-scale SAG mill by comparison with experimental results at the same operating conditions at different mill rotation speeds (rpm).

5. Conclusion

In this research work, an open-source software, LIGGGHTS, was used to perform DEM simulations of industrial-scale SAG mills. Also for the first time, the effects of different mill liner types on two new parameters introduced by the authors, i.e. ‘head height’ and ‘impact zone length’ were investigated. The main innovation and novelty of this paper was introducing and basing these two parameters to evaluate and determine the trajectory of ball motion for investigating the impact mechanism and improving the performance of industrial-scale SAG mills. The following results were obtained:

- 1) In all liner types, cascade motion was observed at both speeds (i.e. 70% and 80% of CS).
- 2) At 70% and 80% of CS, the Smooth and Wave liners did not produce cataract motion. In the other liners, a cataract motion was observed. Also there was centrifugal motion

only for the Ship-lap and Step liners. As a result, some of the balls did not participate in the comminution, and the impact mechanism was reduced.

- 3) According to the data available in Table 4, charge shoulder and toe heights were not suitable criteria for evaluating the mill performance and impact mechanism. In this work, ‘head height’ and ‘impact zone length’ were replaced as appropriate criteria.
- 4) The results obtained indicated that the charge heads were, respectively, about 475.00, 516.40, 873.37, 838.87, 822.39, 877.82, and 810.88 cm at the simulations performed with the Smooth, Wave, Rib, Ship-lap, Lorain, Osborn, and Step liners at 70% of CS. The corresponding values at 80% of CS were as follow: 516.40, 573.76, 901.93, 859.28, 849.31, 931.60, and 828.00 cm. Also the impact zone lengths were, respectively, about 49.72, 74.54, 124.00,

- 115.78, 82.80, 132.21, and 107.54 cm at the simulations performed with the Smooth, Wave, Rib, Ship-lap, Lorain, Osborn, and Step liners at 70% of CS. The corresponding values for impact zone lengths at 80% of CS were as follow: 49.72, 132.21, 173.12, 124.00, 132.21, 205.62, and 115.78 cm.
- 5) At 70% of CS, all liners except the Wave liner had a favorable effect on the impact mechanism. Also the Osborn liner performed best because it increased both the charge head height and the impact zone length. Additionally, the Osborn and Rib liners were recommended for the mill. The Wave liner also lacked the ability to create the right head height and increase of the impact zone length and performed similar to the Smooth liner.
 - 6) At 80% of CS, all liners except Wave had a favorable effect on increasing the charge head height. However, unlike the 70% case, the Wave and Lorain liners also had a relatively favorable effect on increasing the impact zone length. The Osborn and Rib liners had the best performance, and the other liners had a relatively successful performance in increasing the impact zone length. Also the Osborn liner was recommended as the best liner because it increased both the charge head height and the impact zone length.
 - 7) In all cases, the increase in the critical speed increased the charge head height, and thereby, increased the impact mechanism and improved the mill performance. The most positive effect of increasing the mill speed was on the Osborn, Wave, and Smooth liners, respectively.
 - 8) In all cases except the Smooth liner, increasing the mill speed increased the impact zone length, and thereby, improved the impact mechanism and mill performance. Also the most positive effect was related to the Osborn liner.
 - 9) In general, at both critical speeds, the Wave liner had little effect on the charge head height, and the abrasion mechanism was more dominant in it than the other liners, and therefore, it is not recommended to install this liner in the mineral processing plants.
 - 10) Increasing the mill speed in the Smooth liner only increased the charge head height, and did not affect the impact zone length. For the Ship-lap and Step liners, it had little effect on improving the mill performance. In the

Lorain and Rib liners, it had a greater effect on increasing the impact zone length but had a moderate effect on increasing the head height.

- 11) Although the performance of the Wave liner was not desirable, the effect of speed increase was very effective on improving its performance. As a result, this liner performance could be dramatically improved by increasing the mill speed to values above 80% of CS (e.g. 90% or 95% of CS).
- 12) In general, according to all conditions, the Osborn liner is preferred over the Rib liner, and is recommended as the optimal liner in this work.
- 13) In order to validate the simulation results, a laboratory-scale SAG mill was simulated. Comparison of the simulations related to the laboratory-scale SAG mill with the experimental results demonstrated a good agreement, which validated the DEM simulations and the software used.
- 14) Finally, the results obtained indicated that the Osborn liner, due to the angularity of its lifters and their proper number (60 lifters) and thickness (low thickness), performed best because it increased both 'head height' and 'impact zone length' more than the other liners. Thus this liner is recommended as the best and optimal liner in this research work and is suggested for installation inside the industrial SAG mills. Also the Wave liner, due to its specific geometrical shape and its wavy lifters as well as their low number (11 lifters) and inadequate thickness (thick lifters), provided the lowest charge 'head height'. Therefore, it is not recommended to install this liner inside the industrial SAG mills.

Acknowledgments

The authors wish to thank Shahrood University of Technology and Professor Mohammad Ataei for providing the supercomputer required for the DEM simulations.

References

- [1]. Rosales-Marín, G., Andrade, J., Alvarado, G., Delgadillo, J.A. and Tuzcu, E.T. (2019). Study of lifter wear and breakage rates for different lifter geometries in tumbling mill: Experimental and simulation analysis using population balance model. *Minerals Engineering*, 141: 105857.

- [2]. Mishra, B.K. and Rajamani, R.K. (1992). The discrete element method for the simulation of ball mills. *Applied Mathematical Modelling*, 16 (11): 598-604.
- [3]. Powell, M.S. and McBride, A.T. (2004). A three-dimensional analysis of media motion and grinding regions in mills. *Minerals Engineering*, 17 (11-12): 1099-1109.
- [4]. Cleary, P.W. (1998). Predicting charge motion, power draw, segregation and wear in ball mills using discrete element methods. *Minerals Engineering*, 11 (11): 1061-1080.
- [5]. Cleary, P.W. (2001). Charge behaviour and power consumption in ball mills: sensitivity to mill operating conditions, liner geometry and charge composition. *International journal of mineral processing*, 63 (2): 79-114.
- [6]. Cleary, P.W. (2001). Recent advances in DEM modelling of tumbling mills. *Minerals Engineering*, 14 (10): 1295-1319.
- [7]. Cleary, P.W., Morrisson, R. and Morrell, S. (2003). Comparison of DEM and experiment for a scale model SAG mill. *International Journal of Mineral Processing*, 68 (1-4): 129-165.
- [8]. Djordjevic, N., Shi, F.N. and Morrison, R. (2004). Determination of lifter design, speed and filling effects in AG mills by 3D DEM. *Minerals Engineering*, 17 (11-12): 1135-1142.
- [9]. Maleki-Moghaddam, M., Ghasemi, A.R., Yahyaei, M. and Banisi, S. (2015). The impact of end-wall effect on the charge trajectory in tumbling model mills. *International Journal of Mineral Processing*, 144: 75-80.
- [10]. Owen, P. and Cleary, P.W. (2015). The relationship between charge shape characteristics and fill level and lifter height for a SAG mill. *Minerals Engineering*, 83: 19-32.
- [11]. Weerasekara, N.S., Liu, L.X. and Powell, M.S. (2016). Estimating energy in grinding using DEM modelling. *Minerals Engineering*, 85: 23-33.
- [12]. Cleary, P.W. and Owen, P. (2018). Development of models relating charge shape and power draw to SAG mill operating parameters and their use in devising mill operating strategies to account for liner wear. *Minerals Engineering*, 117: 42-62.
- [13]. Hasankhoei, A. R., Maleki-Moghaddam, M., Haji-Zadeh, A., Barzgar, M. E. and Banisi, S. (2019). On dry SAG mills end liners: Physical modeling, DEM-based characterization and industrial outcomes of a new design. *Minerals Engineering*, 141: 105835.
- [14]. Bian, X., Wang, G., Wang, H., Wang, S. and Lv, W. (2017). Effect of lifters and mill speed on particle behaviour, torque, and power consumption of a tumbling ball mill: Experimental study and DEM simulation. *Minerals Engineering*, 105, 22-35.
- [15]. Pedrayes, F., Norniella, J.G., Melero, M.G., Menéndez-Aguado, J. M. and del Coz-Diaz, J. J. (2018). Frequency domain characterization of torque in tumbling ball mills using DEM modelling: Application to filling level monitoring. *Powder Technology*, 323: 433-444.
- [16]. B.A. Wills, T.J. and Napier-Munn. (2016). "Wills' Mineral Processing Technology", 8th edition. Elsevier, pp. 147–180. Chapter 7.
- [17]. Jahani, M., Farzanegan, A. and Noaparast, M. (2015). Investigation of screening performance of banana screens using LIGGGHTS DEM solver. *Powder Technology*, 283, 32-47.
- [18]. Nassauer, B., Liedke, T. and Kuna, M. (2013). Polyhedral particles for the discrete element method. *Granular matter*, 15 (1): 85-93.
- [19]. Raji, A.O. and Favier, J. F. (2004). Model for the deformation in agricultural and food particulate materials under bulk compressive loading using discrete element method. I: Theory, model development and validation. *Journal of food engineering*, 64(3), 359-371.
- [20]. Nassauer, B. and Kuna, M. (2013). Contact forces of polyhedral particles in discrete element method. *Granular Matter*, 15 (3): 349-355.
- [21]. Balevičius, R., Džiugys, A., Kačianauskas, R., Maknickas, A. and Vislavičius, K. (2006). Investigation of performance of programming approaches and languages used for numerical simulation of granular material by the discrete element method. *Computer Physics Communications*, 175 (6): 404-415.
- [22]. Delaney, G. W., Cleary, P.W., Morrison, R.D., Cummins, S. and Loveday, B. (2013). Predicting breakage and the evolution of rock size and shape distributions in Ag and SAG mills using DEM. *Minerals Engineering*, 50, 132-139.
- [23]. Ting, J.M., Khwaja, M., Meachum, L.R. and Rowell, J.D. (1993). An ellipse-based discrete element model for granular materials. *International Journal for Numerical and Analytical Methods in Geomechanics*, 17(9), 603-623.
- [24]. Shmulevich, I. (2010). State of the art modeling of soil–tillage interaction using discrete element method. *Soil and Tillage Research*, 111 (1): 41-53.
- [25]. Cleary, P.W. and Sawley, M.L. (2002). DEM modelling of industrial granular flows: 3D case studies and the effect of particle shape on hopper discharge. *Applied Mathematical Modelling*, 26 (2): 89-111.
- [26]. Munjiza, A. Cleary, P. W. (2009). Industrial particle flow modelling using discrete element method. *Engineering Computations*.
- [27]. Cleary, P.W. and Sinnott, M.D. (2008). Assessing mixing characteristics of particle-mixing and granulation devices. *Particology*, 6 (6): 419-444.

- [28]. Cleary, P.W. (2010). DEM prediction of industrial and geophysical particle flows. *Particuology*, 8 (2): 106-118.
- [30]. Just, S., Toschkoff, G., Funke, A., Djuric, D., Scharrer, G., Khinast, J. and Kleinebudde, P. (2013). Experimental analysis of tablet properties for discrete element modeling of an active coating process. *AAPS PharmSciTech*, 14 (1): 402-411.
- [31]. McBride, W. and Cleary, P.W. (2009). An investigation and optimization of the 'OLDS' elevator using Discrete Element Modeling. *Powder Technology*, 193 (3): 216-234.
- [32]. Goniva, C., Kloss, C., Deen, N.G., Kuipers, J.A. and Pirker, S. (2012). Influence of rolling friction on single spout fluidized bed simulation. *Particuology*, 10 (5): 582-591.
- [33]. Goniva, C., Kloss, C., Hager, A. and Pirker, S. (2010, June). An open source CFD-DEM perspective. In *Proceedings of OpenFOAM Workshop, Göteborg* (pp. 22-24).
- [34]. Kloss, C., Goniva, C., Aichinger, G. and Pirker, S. (2009, December). Comprehensive DEM-DPM-CFD simulations-model synthesis, experimental validation and scalability. In *Proceedings of the seventh international conference on CFD in the minerals and process industries, CSIRO, Melbourne, Australia*.
- [35]. Weerasekara, N.S., Powell, M.S., Cleary, P.W., Tavares, L.M., Evertsson, M., Morrison, R.D. and Carvalho, R.M. (2013). The contribution of DEM to the science of comminution. *Powder Technology*, 248, 3-24.

بررسی تأثیر نوع لاینرهای پوسته بر عملکرد آسیاهای نیمه‌خودشکن صنعتی با استفاده از روش اجزای گسسته

محمد جهانی چگنی*، سجاد کلاهی

دانشگاه صنعتی شاهرود، دانشکده مهندسی معدن، نفت و ژئوفیزیک، شاهرود، ایران

ارسال 2019/10/22، پذیرش 2020/2/7

* نویسنده مسئول مکاتبات: m.jahani1983@gmail.com

چکیده:

نوع لاینرهای پوسته، سرعت چرخش و درصد پرشدگی گلوله‌ها فاکتورهای کلیدی هستند که رفتار بار درون آسیاهای نیمه‌خودشکن و در نتیجه عملکرد آنها را تحت تأثیر قرار می‌دهند. در این تحقیق، عملیات آسیاکنی آسیاهای نیمه‌خودشکن صنعتی با استفاده از روش اجزای گسسته (راگ) مورد بررسی قرار گرفته است. در ابتدا، یک آسیای نیمه‌خودشکن صنعتی با ابعاد 9/5 متر در 4/42 متر که دارای لاینر نوع Smooth است، شبیه‌سازی شده است. سپس با تغییر دادن نوع لاینرها، یعنی لاینرهای Wave، Rib، Ship-lap، Osborn، Lorain، Step و شش شبیه‌سازی مستقل دیگر انجام شده‌اند. به منظور بررسی مکانیزم ضربه و بهبود عملکرد آسیا، دو پارامتر جدید به نام «ارتفاع هد» و «طول زون ضربه» معرفی شده‌اند. سپس تأثیرات نوع لاینرهای پوسته آسیا بر آن پارامترها در دو سرعت مختلف آسیا، یعنی 70 درصد و 80 درصد سرعت بحرانی (CS) آن، ارزیابی شده‌اند. همچنین برای اعتبارسنجی نتایج شبیه‌سازی، یک آسیای نیمه‌خودشکن مقیاس آزمایشگاهی با ابعاد 57/3 سانتی‌متر در 16/0 سانتی‌متر شبیه‌سازی شده است. نتایج به دست آمده نشان می‌دهند که لاینر Osborn، بواسطه زاویه‌دار بودن لیفت‌هایش و تعداد و ضخامت مناسب آن‌ها، به بهترین نحو عمل می‌کند زیرا هر دو پارامتر مذکور را بیشتر از سایر لاینرها افزایش می‌دهد. بنابراین، این لاینر به عنوان بهترین لاینر و لاینر بهینه در این کار تحقیقاتی پیشنهاد می‌شود و برای نصب درون آسیاهای نیمه‌خودشکن صنعتی توصیه می‌گردد. همچنین لاینر Wave، به دلیل شکل هندسی خاص و لیفت‌های موجی شکلش و نیز تعداد کم و ضخامت ناکافی آن‌ها، کمترین «ارتفاع هد» بار را ایجاد می‌کند. بنابراین، این لاینر برای نصب درون آسیاهای نیمه‌خودشکن صنعتی توصیه نمی‌شود. ضمناً، مقایسه شبیه‌سازی‌های مربوط به آسیای نیمه‌خودشکن مقیاس آزمایشگاهی با نتایج تجربی تطابق خوبی را نشان می‌دهد که شبیه‌سازی‌های راگ و نرم‌افزار استفاده‌شده را اعتبارسنجی می‌کند.

کلمات کلیدی: شبیه‌سازی راگ، آسیاهای نیمه‌خودشکن صنعتی، نوع لاینرهای پوسته آسیا، ارتفاع هد، طول زون ضربه.